THE JOURNAL OF PHYSICAL CHEMISTRY B

Article

Cite This: J. Phys. Chem. B XXXX, XXX, XXX−XXX

pubs.acs.org/JPCB

Cooling of Pure Water at Room Temperature by Weak Electric Currents

Iman Rad*,†,‡ and Gerald H. Pollack†

†Department of Bioengineering, University of Washington, Box 355061, Seattle, Washington 98195, United States

‡Stem Cell Technology Research Center, Tehran 1997775555, Iran

ABSTRACT: Flow of electrical current through water is expected to increase water temperature. We passed low-frequency alternating electric current through distilled, deionized water using platinum electrodes and found, instead, a diminution of temperature. The diminution was observed using both an infrared camera and a spectroradiometer, the latter allowing us to obtain spectral information. The diminished temperature persisted for at least half an hour following cessation of the current flow. Diminished radiant energy implies reduced charge displacements, which in turn implies increased structural order. Hence, the passage of charge into water appears to increase the water structure.

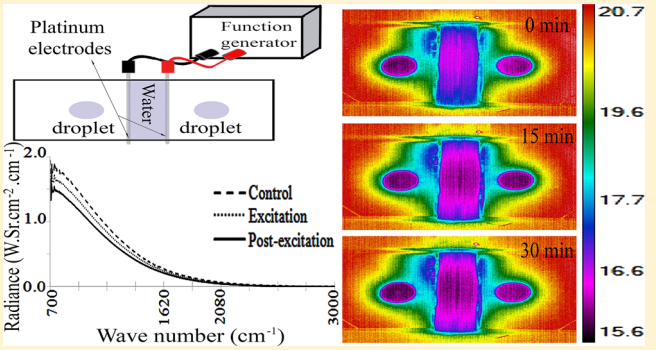

1. INTRODUCTION

Pure water shows inconsistent electrical behavior. In theory, it should exhibit little or no conductivity because of the absence of charge carriers. However, examples exist to show that even pure water can carry current.[1]

Previous work shows that passing direct current between electrodes immersed in pure deionized water establishes charge carriers through electrolysis.[2] A high pH region forms at the negative electrode, whereas a low pH region forms at the positive electrode. This pH gradient may persist for tens of minutes after the current has been turned off. The same occurs in dilute ionic solutions.[3] Hence, the presence of contaminant ions is not the driving force underlying these processes.

Although pure water is presumed to have zero electrical conductivity, some conductivity arises from the electrochemical mobility of the hydrogen and hydroxide ions.[4] On the other hand, when extremely low and high pH regions form around immersed electrodes, the respective regions will become oppositely charged.[2] Hence, pure water may dissociate and get charged or discharged after the electric current turns on and off, respectively.

Here, we reexamined the impact of alternating and direct current flow between electrodes immersed in water. Given the high- and low-pH zones that may persist around current-passing electrodes, we wondered whether those enduring zones might imply some kind of water structuring. We investigated the possibility using a spectroradiometer and an infrared camera.

2. EXPERIMENTAL SECTION

2.1. Experimental Design. Three types of measurements were made. The first was carried out on pure, deionized[5] water with no imposed current flow. It is referred as the "control." The second measurement was carried out with an electric field imposed between electrodes immersed in the water-containing chamber. Current was provided via a function generator (SRS Model DS335). The water was exposed, or in other words, "excited" either with a DC (direct current) or AC (alternative current) electric field at series of frequencies ranging from 0.1 to 45 Hz. Note: the frequency of 7.8 Hz was used instead of 8 Hz because this (Schumann) frequency is reported to have a role in the transduction of biological information into water.[5] The amplitude of the applied voltage was 4.5−7.5 V, and the excitation period extended over 30 min. The third measurement was made after the voltage supply had been turned off. It, too, extended for 30 min and is referred to as the "post-excitation" phase.

During these three periods (control, excitation, and post-excitation), we assessed potential structural changes by measuring the water's radiance as well as its temperature (see below).

2.2. Chamber. All experiments were conducted using a shallow polypropylene dish (4.5 cm width, 2.5 cm length, and 0.5 cm height). Before the experiment began, the chamber was filled with water and left for 30 minutes to become thermally stable. Then, the experiment began. The deionized (DI) water was high-performance liquid chromatography grade, 18.2 MΩ cm—obtained from a standard water purification system (Diamond TII, Barnstead). Platinum wires (Sigma-Aldrich, CAS: 7440-06-4) immersed in water served as electrodes. Application of an electric field between the electrodes created current through the water. The electrical energy needed, in our

Received: December 26, 2017
Revised: June 28, 2018
Published: July 11, 2018

DOI: 10.1021/acs.jpcb.7b12689
J. Phys. Chem. B XXXX, XXX, XXX−XXX

study, for a complete electrolysis of pure water can be calculated to lie between 1.3 and 13 Watt-hour (W-h). By complete electrolysis, we mean the total conversion of water to H_2 and O_2. In our study, the electrolysis rate was almost 10^6 times lower than what was needed for complete hydrolysis. Generally, the amplitude of the current correlated with the applied frequency. In other words, the current amplitude was not set and depended on the applied frequency. When AC was applied with frequencies of 0.1−7.8 Hz, the applied energy to the water was 16.5−22.5 μW-h. Increasing the applied frequency from 11 to 45 Hz maintained the energy at ∼4.05 μW-h. For DC, the applied energy was always 7.5 μW-h.

2.3. Infrared (IR)-Radiance Recording Setup. To assess the structural changes in water, we used an MR170 spectroradiometer, which records the emission spectra in the wavelength range of 2−15 μm (5000−667 cm^{-1}). Raw spectral data come from averaging 100 measurements. The spectra are then calibrated against known sources of black-body radiation. Two black-body references are used. The black bodies must have high emissivity and constant temperature. Hence, the palm of the hand and liquid nitrogen were set as references, representing the minimum and maximum thermal limits that were fed to the device's Fourier-transforming software (FTSW500 Version 1.06).

Calibration sources in general are radiation sources that must have high emissivity and different temperatures—higher or lower than the sample. The palm of the hand satisfies both criteria for the high-temperature reference. Liquid nitrogen was selected as the lower temperature reference with the same logic. Inevitably, the radiance of the thermal reference may vary after a while because of the variation in ambient temperature. Such variation then compromises the reproducibility and precision of the measured radiance. Indeed, one may never have an absolute (constant) reference because of the time variation of the reference radiation. Hence, it is necessary to set a relative reference for each set of measurements. Thus, choosing a thermal reference is generally an arbitrary decision, which very much depends on the condition of the experiment and the scene in which the radiance has to be measured.[6]

The software provides both the amount of radiation (signal) and residuals (noise). The noise represents both the amount of ambient thermal noise and computational error of the measured spectra. The higher the noise amplitude, the lower the expected reproducibility. In our experiments, the calibration residuals were 10 to 20 times lower than the radiance amplitude and could therefore be ignored.

The schematic design of the experiment is shown in Figure 1. To obtain the reproducible radiance patterns from the sample, the water-chamber distance from the radiometer input must be optimized. To achieve the optimal angular acceptance, the water chamber surface was set parallel to the collimator detection path, as recommended by Niclòs et al. in 2005[7] (see Figure 1A, horizontal dotted line). As long as the upcoming water radiation intersects the detection path, there is no further need to direct the radiation to the center of the collimator.

The radiant energy emerging from water during the 30 minutes exposure to the electric field was recorded every 5 minute. The radiated spectra were then averaged after 30 minutes of total measurement time. Each 30 min period is considered as one full time set.

2.4. Infrared Visualization. Besides recording with the spectroradiometer, we also recorded images obtained using an infrared sensing camera (ThermoVision SC-6000—FLIR Systems) located directly above the water chamber. This allowed us to record the infrared radiation emitted from the water surface (Figure 1B), as described by Ienna et al. in 2012.[8] The ThermoVision SC-6000 camera has a spectral sensitivity range between 3 and 5 μm in wavelength (3333−2000 cm^{-1}) and a temperature sensitivity of 50 mK. The camera lens was placed approximately 40 cm above the water. The software used for visualization of the data was ExaminIR 1.2.0.1076 (FLIR Systems). In these IR experiments, the chamber was not completely filled with water. Instead, only half a milliliter of DI water was poured between the two parallel platinum electrodes that had been installed in the chamber. The water did not extend beyond those electrodes. However, as a control for measuring evaporation rate, two drops of water (each with volume of 200 μL) were placed on the chamber floor beyond the platinum electrodes (Figure 1B,C). Droplet volume did not diminish measurably during one hour of experimentation. Concern over possible evaporative effects was the main reason why the experiment was set for only one hour.

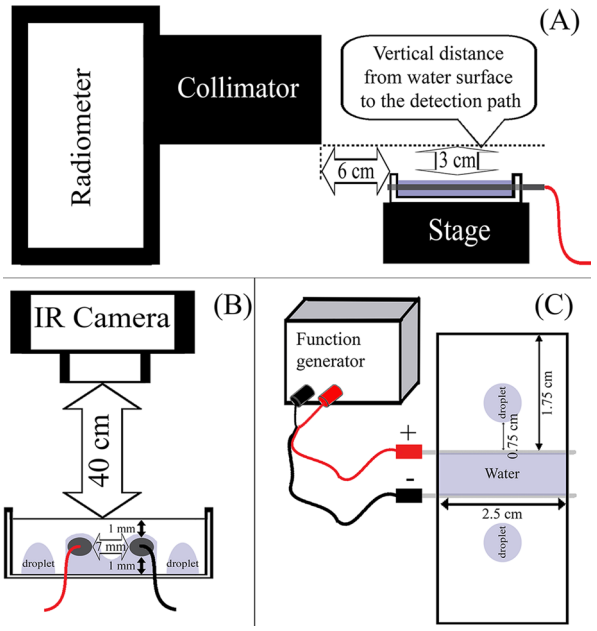

Figure 1. Schematic views of the measurement setup. (A) Lateral view of spectroradiometer and water chamber, resting on stage. (B) Front view showing IR camera and cross section of the water chamber including electrodes and droplets. (C) Top view of water chamber used with IR camera. It should be noted that in IR-camera monitoring experiments, the water exists only between electrodes, whereas in the spectroradiometer experiment, the chamber is filled with water. Red and black wires represent positive and negative poles, whereas the attached gray lines in (C) represent platinum wires. Drawing not to scale.

3. RESULTS

In this study, water was excited for 30 minutes with either alternative or direct currents. We observed the consequences during the period of excitation and during the 30 minutes period of post-excitation. The post-excitation monitoring period was short enough to avoid interference from surface evaporation but long enough to judge the impact of excitation. Both excitation and post-excitation periods were monitored by a spectroradiometer and an IR camera.

DOI: 10.1021/acs.jpcb.7b12689
J. Phys. Chem. B XXXX, XXX, XXX−XXX

3.1. Interpreting Radiometric Spectral Changes. In examining the excitation and postexcitation spectra, we first tested for the persistence of changes initiated during the excitation period. The higher the persistence during the post-excitation period, the stronger the implication of lasting structure. Second, we examined how closely the spectra correlate with the applied treatment.

3.2. Comparison of Water Radiance in Excitation and Postexcitation Periods. Figure 2 shows the radiance spectra

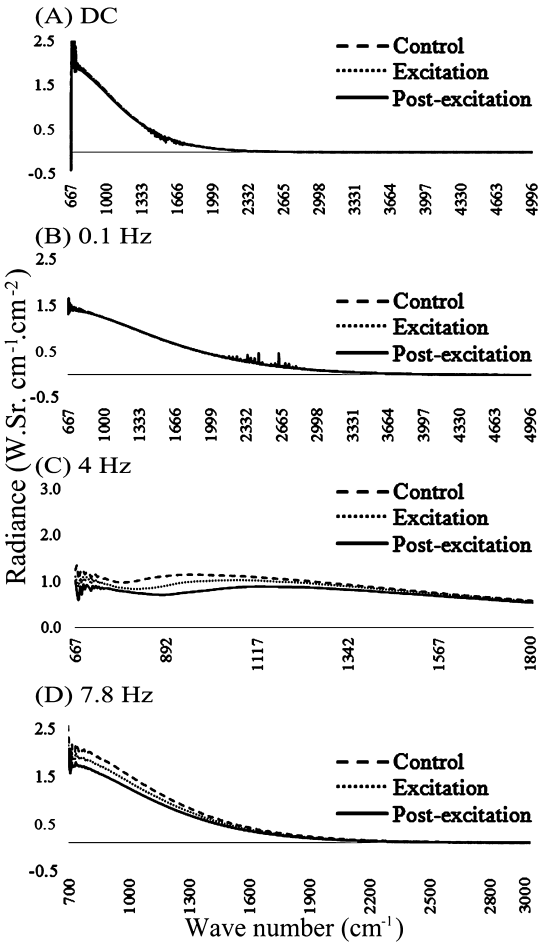

Figure 2. Radiance of water during and after application of DC and low-frequency currents. The figures are radiometric spectra calculated against black-body references. All amplitudes should be multiplied by e^{-5}. The SI units of radiance are commonly expressed as Watts per steradian per square centimeter per centimeter ($W \cdot Sr^{-1} \cdot cm^{-1} \cdot cm^{-2}$). Although DC and 0.1 Hz caused no obvious change, 4 and 7.8 Hz lowered the radiance after exposure.

obtained during control, excitation, and post-excitation periods. Application of DC or 0.1 Hz frequency created a little obvious change from control (Figure 2A,B). By increasing the applied frequency to 4 and 7.8 Hz, water radiance dropped appreciably during both excitation and post-excitation periods at 667–1800 cm^{-1} (15–5.55 μm) and 700–3000 cm^{-1} (14.3–3.3 μm), respectively, compared to control (Figure 2C,D). The corresponding measured noise (not shown) was very close to zero in all samples.

Increasing the applied frequency to 11 and 14 Hz lowered the post-excitation radiance of water over a narrower range, at 1000–3000 cm^{-1} (10–3.33 μm) and 1000–4000 cm^{-1} (10–2.5 μm), respectively (Figure 3A,B). When higher frequencies

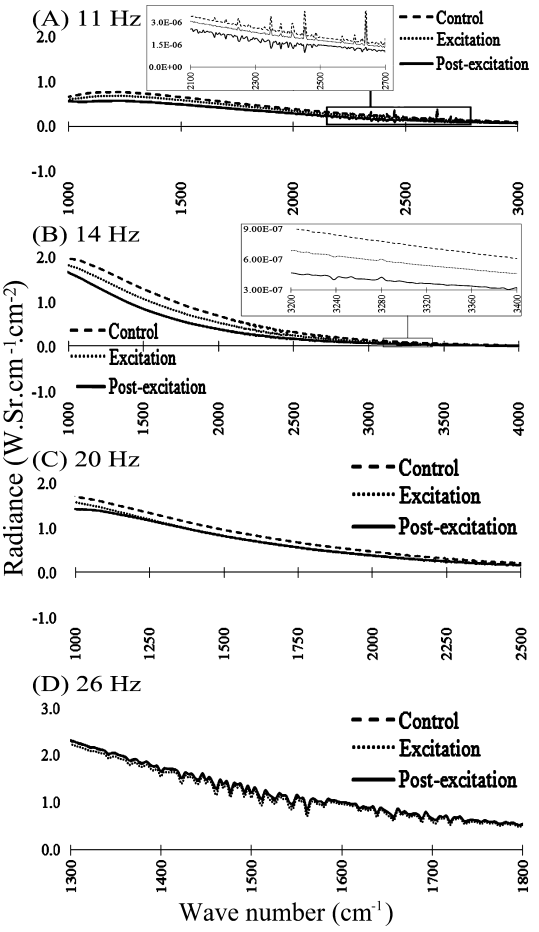

Figure 3. Water radiance profiles during and after exposure to alternative currents at higher frequencies. All radiance amplitudes must be multiplied by e^{-5}. Note that the *x*-axis scale needs to remain selective. It was not applicable to show a unified *x*-axis for all graphs because the relevant changes occur in different regions of the spectrum for each applied frequency. Showing the entire spectrum (667–5000 cm^{-1}) on each graph also makes it look similar to a zoomed-out graph with poor visual recognition.

of 20 and 26 Hz were applied, the lowered radiance during excitation and post-excitation periods occurred at even narrower ranges, of 1000–2500 (10–4 μm) and 1300–1800 cm^{-1} (7.69–5.55 μm), respectively (Figure 3C,D).

Figure 3 shows the results obtained at higher frequencies. At frequencies ranging from 11 to 26 Hz, water radiance in the post-excitation period remained lower than either the control or the excitation period. The corresponding noise was, again, close to zero. When frequencies of 33, 39, and 45 Hz (not shown) were applied, the water radiance during excitation and post-excitation was not different from control.

3.3. Correlation Between Applied Current and Thermal Radiance. The progressive lowering of radiance with excitation was unexpected. With current flow at 4, 7.8, 11, and 14 Hz, the radiance loss after first 8–10 min of excitation continued with a linear trend beyond the excitation period until the end of the postexcitation period. This phenomenon was not observed with DC excitation or when frequencies lower than 4 Hz and higher than 20 Hz were applied.

3.4. IR Visualization. We attempted to see whether this reduction of radiant energy might correlate with lowering of the sample temperature using an IR camera.

DOI: 10.1021/acs.jpcb.7b12689
J. Phys. Chem. B XXXX, XXX, XXX–XXX

When water is poured between electrodes and two droplets are set beyond those electrodes, water temperatures may vary over time. To measure the thermal variation, water temperature was monitored for one hour without any current flow between electrodes. This monitoring could be considered as a thermal control for further experiments. We found that the temperature in the water between electrodes was stable except for the first 10−15 min (Figure 4). In other words, after the initial transient, the effect of evaporation was practically nil.

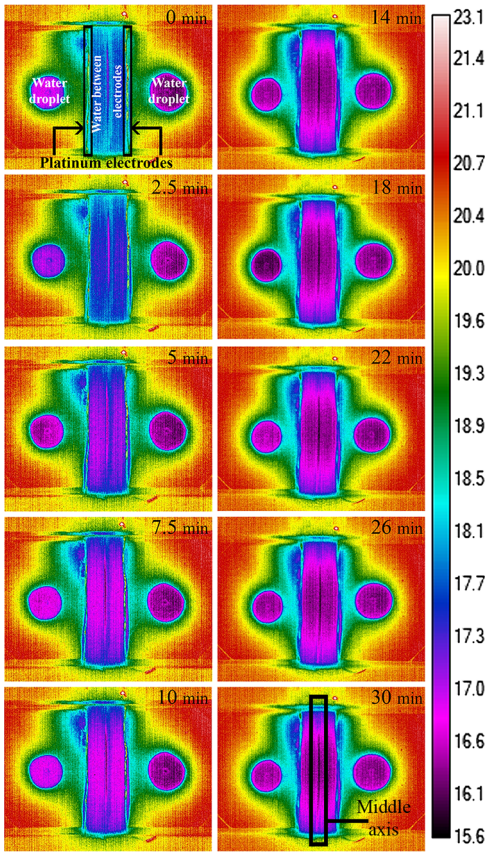

Figure 4. Thermal equilibration of water following the positioning of water between the two parallel platinum electrodes and control droplets beyond the electrodes. No current was applied. The left column shows appreciable drop of temperature between the electrodes during first 10 minutes, whereas the right column shows stable water temperature during the next 20 minutes. The times of snapshots are shown at the top right corner of each panel. Temperature calibration is provided at the right side of the figure. The "middle axis" could be always observed, but at 30 min, it finally became stable and is highlighted inside the black rectangle.

To double check for any substantive evaporative and thermal fluctuation effects, water droplets were put beyond the electrodes. This was carried out at the same time that water was placed between electrodes. After 10−15 minutes, all thermal variations in droplets and inter-electrode water vanished. During the next 20 minutes, water temperatures remained thermally stable. We therefore opted to wait for one hour of equilibration before beginning actual experiments. During that period, the middle area of water between two electrodes also showed the most diminution in temperature compared to the surroundings.

We refer to just the line in the middle between electrodes as the "middle axis". Figure 1B illustrates that the water between electrodes has the least thickness compared to its surrounding water that faces the electrodes. This area of diminished thickness in Figure 1B corresponds to the lower temperature "middle axis" in Figure 4. Because 1 h of temperature and evaporation control showed that thermal variation mostly stops by 15 min, samples were left for half an hour to equilibrate, after which the experiments began.

3.5. Temperature Changes during Application of Current. When we applied AC or DC, not only did water fail to heat up but it dropped in temperature by about 2 K (Figure 5). The dynamics of the drop depended on frequency. The

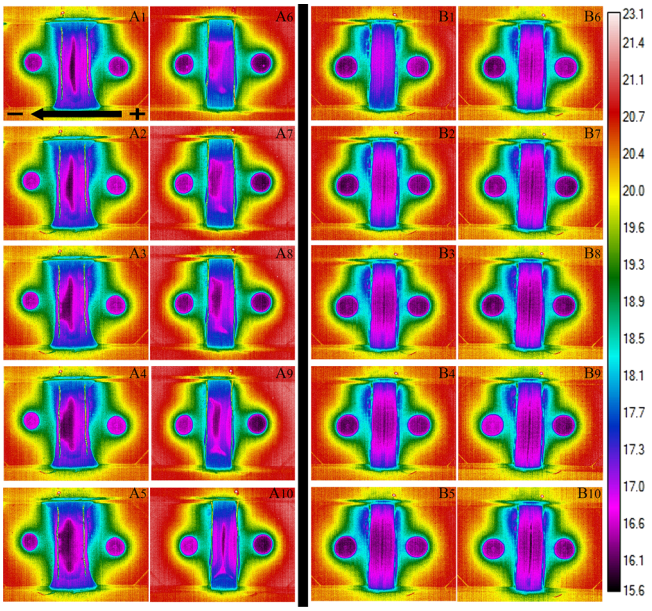

Figure 5. Water thermal profiles during and following 4.5 V DC (A) and 7.8 Hz AC (B) treatments. Successive panels separated by 6 min intervals. Panels 1−5 and 6−10 represent excitation and post-excitation periods, respectively. The direction of electric field in DC panel is from right to the left, as shown by the black arrow. Note the partial restoration of water temperature during post-excitation period (A_6 to A_{10}). For AC results (panel B), note the thermal drop of water temperature during excitation (B_1 to B_9) that continues to the post-excitation periods (B_6 to B_{10}). Contrary to the temperature restoration at post-excitation of the DC treatment, the drop of temperature is preserved during post-excitation when AC is applied.

figure shows that the cooling effect at frequencies of 4−26 Hz started after some delay compared to DC. At frequencies higher than 26 Hz (33, 39, and 45 Hz), or lower than 4 Hz (0.1 Hz), including DC, there was no difference between excitation and post-excitation temperatures. When frequencies between 4 and 26 Hz were applied, the average water temperature during the post-excitation period diminished further than during the excitation period.

3.6. Comparative Trend of Temperature Variation in AC and DC Treatments. An interesting finding, with DC treatment, was the gradual shift of the low-temperature region around the "middle axis" of water toward the negative electrode (Figure 5A_1−A_5).[2] This shift was reversible: it restored itself to its initial shape and position during the 30 minutes of post-excitation (Figure 5A_6−A_{10}). The most dramatic shift was observed during 6−12 minutes after excitation began (Figure 5A_1,A_2) and after post-excitation began (Figure 5A_6,A_7).

DOI: 10.1021/acs.jpcb.7b12689
J. Phys. Chem. B XXXX, XXX, XXX−XXX

The drop of temperature in AC-treated water was more homogenous and less dramatic (Figure 5B_1−B_5) compared to the DC-treated water (Figure 5A_1−A_5) at the same voltage.

During DC excitation, an abrupt diminution of temperature occurred during the first 10 minutes (Figure 5A_1,A_2). The temperature became more stable after 10 minutes and remained almost constant up to 30 min (Figure 5A_3−A_5).

During post-excitation, the results differed depending on whether the treatment was AC or DC. For example, following DC treatment (Figure 5A_6−A_7) and 0.1 Hz treatment, the water temperature rose abruptly toward the initial temperature during the first 10 minutes. This rise mirrors the dramatic drop during the excitation period (Figure 5A_1,A_2). With alternative current, however, the drop occurring during excitation persisted up to the end of the post-excitation period.

3.7. Differential Temperature Index. To emphasize the subtle differences between the excitation and post-excitation periods, a new method of data processing was applied. In this approach, the average temperature of water during excitation and post-excitation periods were subtracted from the corresponding control temperature, the latter taken after the initial 30 min equilibration period without treatment. This procedure created two sets of indices for all of treatment time courses. We refer to them as "differential temperature indices (DTIs)". Larger DTI means larger drop in temperature with respect to the control.

For DC treatment, the average DTI during 30 minutes of excitation and post-excitation was similar to AC treatment when current with frequencies of 0.1, 26, 33, 39, and 45 Hz were applied (Figure 6). However, at other frequencies (i.e., 4, 7.8, 11, 14, and 20 Hz), the average DTI index of post-excitation was always larger than that of excitation (Figure 6), implying a continuing drop of temperature.

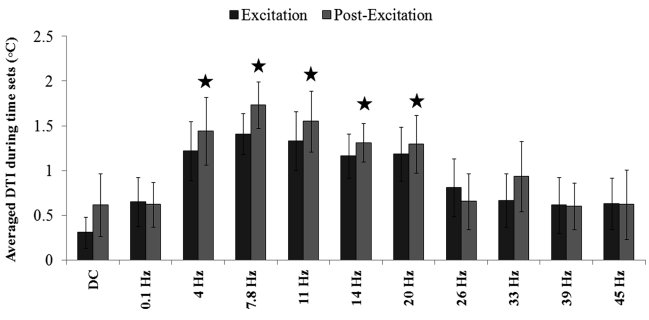

Figure 6. Averaged DTI indices of different treatments. The stars above the post-excitation averages represent a significance of difference compared to the corresponding excitation average. Standard errors represent deviation from the mean.

4. DISCUSSION

We found a reduction of thermal radiance associated with the current flow. This was observed both with a radiometer (Figures 2 and 3) and with an IR camera (Figures 4 and 5). Current flow is generally expected to produce heating but the passage of current through water caused cooling. Hydrolysis of water can cause ionic currents to flow through the experiment cell. The level of hydrolysis in this study, on the order of microamperes, was 10^6 times less than that required for the complete hydrolysis and far below that needed to account for the temperature drop. In the following paragraphs, we discuss the possible mechanisms for explaining the observed temperature drop.

We looked particularly at frequencies ranging between 4 and 20 Hz because both radiometric and IR camera results confirm that application of such alternative currents at certain low frequencies will reduce the water temperature significantly. By applying 4 Hz AC on water, we observe a radiance drop in the 667−1800 cm^{-1} range of the spectrum. Increasing the applied frequency to 7.8, 11, and 14 Hz results in a radiance drop over a broader area of the spectrum, in the ranges of 700−3000, 1000−3000, and 1000−4000 cm^{-1}, respectively. The wider range of diminished radiance indicates that more molecular interactions are involved in the lowered kinetic energy. This thermal response of water persists for at least half an hour and implies long-range structural reconfiguration in water. The global electromagnetic waves at the extremely low frequency (ELF) spectral range with a frequency of 3−60 Hz are named after the physicist Winfried Otto Schumann. These are reported to have certain biological impacts[9] and also play a role in imprinting properties in water and cells.[5,10]

These reports triggered an interest in verifying the effects of ELF alternating currents (AC) on water. Comparison of our results with previous reports shows that the electrified water shares similarities with exclusion-zone[7] water[3] and low-density water.[11] In the following paragraphs, we detail the arguments for this interpretation.

4.1. How Pure Water's Thermal Radiance is Connected to its Electric Charge Index. Water pH, temperature, and electrical conductivity are correlated with each other. Bulk-water pH rises moderately, whereas its electrical conductivity drops as the temperature drops from 303 to 273 K.[12] Hence, with a small drop of temperature, we expect that bulk water will get slightly more basic (more negatively charged) and have lower conductivity. This assumption is based on the fact that the OH^- and H^+ concentrations do not decrease in equal amounts at lower temperatures.[12] An increased ratio of OH^- to H^+ at lower temperature facilitates the formation of electric dipoles, which can then coherently interact with the external radiation fields, resulting in ordered structures in macroscopic domains of a few hundred microns.[13] We do not imply that the lower temperature necessarily occurs because of the negative charge. Rather, the vast majority of regions showing these features, that is, exclusion zones (EZs), have a negative charge.[14]

The correlation between electrical conductivity and temperature is impressively observed in the "middle-axis" area. Regarding the middle-axis shift to the negative electrode after the application of DC, we need to keep in mind that the middle-axis water has lower height than the water next to the electrodes. A lateral view of the water between the electrodes shows a concave shape. The shallow height of the middle axis makes it behave similar to capillary water, which then results in higher surface tension compared to the water near the two electrodes.[15] Hence, shift of the middle axis to the negative electrode may well be related to the difference in surface tension of the two regions.[16] The difference in surface tension probably originates from the complex pattern of charge distribution in the middle-axis area, which then facilitates the middle-axis shift in the same direction as the applied direct electric current.

Timing the water's thermal variation either in the form of spectral radiance or IR radiation depends on the applied frequency. After the application of frequencies lower than 4 Hz

DOI: 10.1021/acs.jpcb.7b12689
J. Phys. Chem. B XXXX, XXX, XXX−XXX

and higher than 20 Hz, most of the temperature loss (DTI increase) and radiance drop occur during the first 10−20 minutes of excitation. The timing patterns of these thermal variations share a similarity with the timing pattern of the charging pure water, as reported by Ovchinnikova et al.[3] Hence, during the time that pure water gets charged either by DC or AC (via frequencies outside of the 4−20 Hz range), it also gets cooler, implying that these processes might be coincidental.

Water's persisting thermal drop in the post-excitation period shares similarity with the persistently cooler EZ water. In the same way, as mentioned earlier, application of electric current builds EZs, which are generally negatively charged.[2,3] The treated water with AC frequencies (between 4 and 20 Hz) loses its radiance even over 10 minutes after the function generator has been turned off. This phenomenon is also expressed by the rise of DTI during the post-excitation period (Figure 6) with an average 1.11 ± 0.42 K temperature drop. This trend of temperature loss in water that is accompanied by accumulation of negative charge and diminution of conductivity could be a manifestation of the increasing EZ water.

4.2. Alternative Mechanism for Persistent Cooling. Another possible explanation for the persistently lowered radiance profile of treated water with AC frequencies of 11 and 14 Hz has to do with reformation of internal hydrogen bonding. In the following paragraphs, we consider it in more detail.

Two different populations of water, low-density water (LDW) and high-density water (HDW), have been identified to be preponderant at temperatures 277.15 and 298.15 K, respectively.[11] They are detected with absorbance peaks at 3300 and 3500 cm^{-1}, respectively.[11] Fluctuating equilibrium between the two types of local structures is driven by incommensurate requirements for minimizing enthalpy (LDW) and maximizing entropy (HDW). The extreme differences anticipated in the hydrogen-bonding environment surprisingly remain the same in bulk water even under conditions ranging from ambient to near the boiling point.[17]

The rotational or bending movements of the hydrogen atom around or along its axial bond with oxygen are reflected in IR absorption spectra at 1644 and 2127 cm^{-1} (6 and 4.7 μm).[18] There are a series of peaks at 2100−2700 cm^{-1} in the control water (Figure 3A) that disappeared when the water was excited at 11 Hz and also remain reduced in the post-excitation water (Figure 3A). Water in the 11 Hz post-excitation period is therefore expected to have generally higher entropy, which comes with a larger number of less structured internal hydrogen bonding nets than control.

Application of 14 Hz current is accompanied by an increase in LDW according to the changing radiation profile at 3200−3400 cm^{-1} during excitation and post-excitation periods (Figure 3B—the zoomed-in rectangle). This difference in radiance could be an indication of the increased LDW formation relative to HDW formation at 14 Hz excitation and post-excitation periods relative to control water. However, it is worth mentioning that the emergence of an LDW-like structure could be a consequence of the minor temperature drop in water after treatment with 14 Hz alternating current.

5. CONCLUSIONS

Application of ELF current makes pure water cooler rather than warmer. The induced cooling implies a structural change that produces more order (crystallinity), which in turn radiates less. We have offered two possible interpretations, one involving LDW and the other involving EZ water, which has been studied extensively in this laboratory. EZ, similar to LDW, has different density than the bulk phase and persists for some time. It also radiates less than bulk water. Hence, EZ water stands as a good candidate to explain the reduced radiance of water.

AUTHOR INFORMATION

Corresponding Author

*E-mail: rad@strc.ac.ir, radi@u.washington.edu (I.R.).

ORCID

Iman Rad: 0000-0002-7185-6629

Notes

The authors declare no competing financial interest.

ACKNOWLEDGMENTS

We thank the Software AG foundation (SAGST) for the support of this work. The authors thank Dr. Vahid Salari and Dr. Rainer Stahlberg for their useful comments.

REFERENCES

(1) Krbal, M.; Stepanek, J.; Wasserbauer, V.; Orsagova, J.; Sumec, S. Floating water bridge phenomenon high voltage laboratory experiments, Electric Power Engineering (EPE), 2017. *18th International Scientific Conference on IEEE*, 2017; pp 1−4.

(2) Klimov, A.; Pollack, G. H. Visualization of charge-carrier propagation in water. *Langmuir* **2007**, *23*, 11890−11895.

(3) Ovchinnikova, K.; Pollack, G. H. Can water store charge? *Langmuir* **2009**, *25*, 542−547.

(4) Light, T. S.; Licht, S.; Bevilacqua, A. C.; Morash, K. R. The fundamental conductivity and resistivity of water. *Electrochem. Solid-State Lett.* **2005**, *8*, E16−E19.

(5) Montagnier, L.; Del Giudice, E.; Aïssa, J.; Lavallee, C.; Motschwiller, S.; Capolupo, A.; Polcari, A.; Romano, P.; Tedeschi, A.; Vitiello, G. Transduction of DNA information through water and electromagnetic waves. *Electromagn. Biol. Med.* **2015**, *34*, 106−112.

(6) Song, X.; Xue, C.; Zhou, K. MR170 type IR Radiometer Calibration Technology; Atlantis Press, 2015.

(7) Niclòs, R.; Valor, E.; Caselles, V.; Coll, C.; Sánchez, J. M. In situ angular measurements of thermal infrared sea surface emissivity—Validation of models. *Remote Sens. Environ.* **2005**, *94*, 83−93.

(8) Ienna, F.; Yoo, H.; Pollack, G. H. Spatially resolved evaporative patterns from water. *Soft Matter* **2012**, *8*, 11850−11856.

(9) Marciak-Kozlowska, J.; Kozlowski, M. On the Interaction of the Schumann Waves with Human Brain. *Journal of Consciousness Exploration & Research* **2017**, *8* (2), 160−167.

(10) Montagnier, L.; Aïssa, J.; Capolupo, A.; Craddock, T.; Kurian, P.; Lavallee, C.; Polcari, A.; Romano, P.; Tedeschi, A.; Vitiello, G. Water Bridging Dynamics of Polymerase Chain Reaction in the Gauge Theory Paradigm of Quantum Fields. *Water* **2017**, *9*, 339.

(11) Maréchal, Y. The molecular structure of liquid water delivered by absorption spectroscopy in the whole IR region completed with thermodynamics data. *J. Mol. Struct.* **2011**, *1004*, 146−155.

(12) Light, T. S. Temperature dependence and measurement of resistivity of pure water. *Anal. Chem.* **1984**, *56*, 1138−1142.

(13) Del Giudice, E.; Preparata, G.; Vitiello, G. Water as a free electric dipole laser. *Phys. Rev. Lett.* **1988**, *61*, 1085.

(14) Zheng, J.-m.; Chin, W.-C.; Khijniak, E.; Khijniak, E., Jr; Pollack, G. H. Surfaces and interfacial water: evidence that hydrophilic surfaces have long-range impact. *Adv. Colloid Interface Sci.* **2006**, *127*, 19−27.

(15) Petersen, P. B.; Saykally, R. J. On the nature of ions at the liquid water surface. *Annu. Rev. Phys. Chem.* **2006**, *57*, 333−364.

(16) Chaplin, M. Theory versus experiment. What is the charge at the surface of water? *Multidisciplinary Research Journal* **2009**, *2*, 1−28.

DOI: 10.1021/acs.jpcb.7b12689
J. Phys. Chem. B XXXX, XXX, XXX−XXX

(17) Huang, C.; Wikfeldt, K. T.; Tokushima, T.; Nordlund, D.; Harada, Y.; Bergmann, U.; Niebuhr, M.; Weiss, T. M.; Horikawa, Y.; Leetmaa, M. The inhomogeneous structure of water at ambient conditions. *Proc. Natl. Acad. Sci. U.S.A.* **2009**, *106*, 15214−15218.
(18) Kim, H.; Kosuda, K.; Van Duyne, R. P.; Stair, P. C. In-Situ Characterization of Heterogeneous Catalysts Themed Issue. *Chem. Soc. Rev.* **2010**, *39*, 4820−4844.

DOI: 10.1021/acs.jpcb.7b12689
J. Phys. Chem. B XXXX, XXX, XXX−XXX